Mathematical Biosciences and Engineering

MBE, 20(2): 2908–2919.
DOI: 10.3934/mbe.2023137
Received: 12 September 2022
Revised: 14 November 2022
Accepted: 24 November 2022
Published: 01 December 2022

http://www.aimspress.com/journal/MBE

Research article

Dynamics of a two-layer neuronal network with asymmetry in coupling

Sridevi Sriram[1], Hayder Natiq[2], Karthikeyan Rajagopal[3], Ondrej Krejcar[4,5,6] and Hamidreza Namazi[4,7,8,*]

[1] Centre for Computational Biology, Chennai Institute of Technology, Chennai 600069, India
[2] Department of Computer Technology Engineering, College of Information Technology, Imam Ja'afar Al-Sadiq University, Baghdad 10001, Iraq
[3] Centre for Nonlinear Systems, Chennai Institute of Technology, Chennai 600069, India
[4] Center for Basic and Applied Research, Faculty of Informatics and Management, University of Hradec Kralove, Hradec Kralove, Czechia
[5] Institute of Technology and Business in Ceske Budejovice, Ceske Budejovice, Czechia
[6] Department of Biomedical Engineering and Measurement, Faculty of Mechanical Engineering Technical University of Kosice, Slovakia
[7] School of Engineering, Monash University, Selangor, Malaysia
[8] College of Engineering and Science, Victoria University, Melbourne, Australia

* **Correspondence:** Email: Hamidreza.namazi@monash.edu.

Abstract: Investigating the effect of changes in neuronal connectivity on the brain's behavior is of interest in neuroscience studies. Complex network theory is one of the most capable tools to study the effects of these changes on collective brain behavior. By using complex networks, the neural structure, function, and dynamics can be analyzed. In this context, various frameworks can be used to mimic neural networks, among which multi-layer networks are a proper one. Compared to single-layer models, multi-layer networks can provide a more realistic model of the brain due to their high complexity and dimensionality. This paper examines the effect of changes in asymmetry coupling on the behaviors of a multi-layer neuronal network. To this aim, a two-layer network is considered as a minimum model of left and right cerebral hemispheres communicated with the corpus callosum. The chaotic model of Hindmarsh-Rose is taken as the dynamics of the nodes. Only two neurons of each layer connect two layers of the network. In this model, it is assumed that the layers have different coupling strengths, so the effect of each coupling change on network behavior can be analyzed. As a result, the projection of the nodes is plotted for several coupling strengths to investigate how the asymmetry coupling influences the network behaviors. It is observed that although no coexisting

attractor is present in the Hindmarsh-Rose model, an asymmetry in couplings causes the emergence of different attractors. The bifurcation diagrams of one node of each layer are presented to show the variation of the dynamics due to coupling changes. For further analysis, the network synchronization is investigated by computing intra-layer and inter-layer errors. Calculating these errors shows that the network can be synchronized only for large enough symmetric coupling.

Keywords: multi-layer networks; asymmetry coupling; neuronal network; synchronization; attractor

1. Introduction

Brain performance analysis is one of neuroscience's most critical aspects. Understanding how the brain works and diagnosing its disorders can be improved by studying the neurons' behaviors. In the brain, the activities of neurons and their interactions produce a wide range of collective phenomena such as partial synchronization (i.e., cluster synchronization and chimera states [1,2]), complete synchronization [3], and spiral waves [4,5]. Generally, in the network of oscillations, synchronization can be affected by changes in the system, such as changes in temperature, external stimuli, or coupling strength [6–8]. Scientists, however, are interested in maintaining synchronization when network criteria change, for example, its dimension [9,10]. Numerous studies deal with the synchronization of neurons [11–13]. This phenomime has been widely studied as it plays a crucial role in brain activities, such as attention, working memory, learning, etc. [14,15]. A network science approach and graph theory can be useful in examining brain behavior. In most mental disorders, abnormalities in neural synchronization have been seen. Patients with schizophrenia are diagnosed with abnormalities in neural synchronization in the gamma range (30–50 Hz) [16], while those with Major Depression are diagnosed with disruptions in spontaneous alpha-band (8–12 Hz) synchrony [17]. Interpersonal neural synchronization is also observed among people when they cooperate. As observed in [18], such synchronization is higher among people who are solving a puzzle in a group (joint attention) rather than completing that puzzle individually (individual attention).

In graph modeling, nodes represent units, and links represent their connections [19]. Brain units can refer to single neural cells, groups of neurons, or cortical brain regions. Also, the connectivity can reflect physical connections between neurons, known as structural connectivity or functional connectivity, which refers to an indirect interaction between different brain regions. Different types of brain imaging can reveal these connections. For instance, the diffusion weighted imaging (DWI) technique indicates structural connectivity in the brain [20], and the functional magnetic resonance imaging (fMRI) technique shows functional connectivity [21].

Due to recent computational advances, many studies have been conducted to analyze the functional and structural characteristics of the brain [22]. In several studies, functional and anatomical asymmetry has been evident in the brain [23]. Different human criteria like gender [24] also contribute to these asymmetry patterns. As an example, anatomical asymmetry in the Sylvian fissure has been detected [25]. It has been shown that men are more likely to display this asymmetry among right-handed people than women, while vice versa is true for left-handers [26]. Besides, it has been shown that the brain exhibits asymmetries in dyslexic children [27], schizophrenic patients [28], and those with Alzheimer's disease [29]. In most cases, these asymmetrical patterns were found between the hemispheres. Other asymmetry effects in dynamical networks have also been examined [30]. Medeiros

et al. [31] used asymmetry coupling to show that an ecological network becomes ordered through asymmetric coupling.

Although several studies have represented the brain as a single network [32], developing some powerful theoretical frameworks like higher-order networks [33] and multi-layer networks [34] in recent years has offered a complete representation of the brain. Multi-layer networks can represent each aspect of the brain through a different layer. For instance, in [35], each functional and anatomical connectivity was considered as one layer of a multi-layer network to investigate the brain's multiplex motifs. Hence, recently, more attention has been paid to multi-layer neuronal networks [36]. Some studies have considered the brain as a multiplex network framework in which information of the specific frequency band is encoded in one layer [37]. From another perspective, based on the cerebral cortex data, each brain hemisphere can be seen as one layer of a multi-layer network. For instance, in [38], such a model was chosen to investigate how matching a network's structural and dynamical parameters lead to the formation of chimera states in the brain.

In light of the above studies, here, a two-layer network of neuron models is considered to investigate asymmetric coupling strength effects on the network behavior and neurons' dynamics. This multi-layer model indicates that asymmetry in coupling strength results in an asymmetry in the trajectories of layers. The result is obtained by analyzing the phase space projections of nodes and plotting bifurcation diagrams of a single node of each layer by changing the coupling strength. Furthermore, computing intra-layer and inter-layer errors of the network demonstrates that it can be synchronized with large enough symmetric coupling strengths.

In this paper, the model is described in Section 2, and its obtained results are mentioned in Section 3. In this section, some trajectories of symmetric and asymmetric coupling are plotted to examine the effect of these couplings on the neurons' dynamics. To quantify the synchronizability of the multi-layer network, the error between and within layers is computed. Finally, the conclusion is drawn in Section 4.

2. Model

Here, a two-layer neuronal network is considered where each layer is a ring of 10 nodes, also known as a double-chain network. This structure is used as a minimal model for the brain hemispheres connected through the corpus callosum. The model schematic is represented in Figure 1. As the node's dynamics, the Hindmarsh-Rose (HR) model is utilized. Here, the mathematical form of this model has been described in Eq (1).

$$\begin{aligned}&\{\dot{v}_{L,m} = u_{L,m} + 3 \times v_{L,m}^2 - v_{L,m}^3 - w_{L,m} + I + C\,\dot{u}_{L,m} = \\ &1 - 5 \times v_{L,m}^2 - u_{L,m}\,\dot{w}_{L,m} = -r \times w_{L,m} + r \times s \times \left(1.6 + v_{L,m}\right)\end{aligned} \tag{1}$$

In this model, $v_{L,m}$ represents the axon membrane potential of the m-th neuron in the layer L, where $L = 1, 2$ and $m = 1, 2, \ldots, 10$. Also $u_{L,m}$ and $w_{L,m}$ are the spiking and bursting variables of that node, respectively. Here $C = c_w + c_b$ represents two types of coupling; within layers (c_w) and between layers (c_b), which are defined by Eq (2) [31]. The coupling is considered as:

$$c_w = \left(v_{L,(m-1)} + v_{L,(m+1)} - 2 \times v_{L,k}\right) \times \sigma_L \tag{2-a}$$

$$c_b = (\sigma_{L'} \times v_{L',m'} - \sigma_L \times v_{L,m}) \times A_{mm'} \tag{2-b}$$

In Eq (2), σ is the coupling strength or synaptic strength between neurons where subscripts L and L' define the layer L and the opposite one, respectively. The adjacency matrix A indicates the connections between the nodes of each layer. Hence, in our model $A_{mm'} = 1$ for $m, m' = \{5,6\}$.

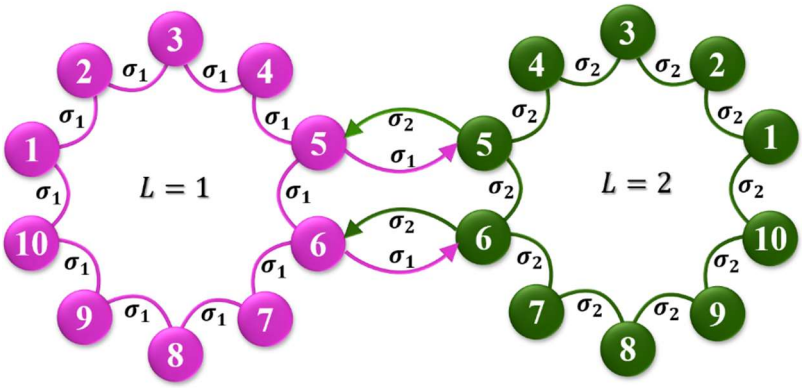

Figure 1. The schematic of the two-layer neuronal network. Layers correspond to brain hemispheres connected to each other by the corpus callosum. Each layer contains 10 nodes connected in a ring structure, making the network similar to a double-chain network.

3. Results

Here, the effects of asymmetric coupling on network dynamics are analyzed. As the couplings are alternated, the neurons' behaviors in each layer are examined. First, one coupling strength remains constant, and the network dynamics are analyzed in phase space based on variations of the other coupling strength. Next, by choosing one coupling as a bifurcation parameter, bifurcation diagrams of one node in each layer are plotted to see the variation of the network dynamics due to asymmetric coupling. In the end, intra-layer and inter-layer synchronization errors are calculated to investigate the effects of asymmetric coupling.

Using $r = 0.006$, $s = 4$, and $I = 3.2$ in Eq (1), each neuron results in chaotic oscillations when $C = 0$, which means there is no coupling among nodes. Notice that HR does not have any coexisting attractor. Nevertheless, as the coupling asymmetry increases, different attractors emerge. To show this phenomenon, some projections of nodes are illustrated in Figure 2 for $\sigma_1 = 10$ and variable σ_2, whereas those of $\sigma_2 = 10$ with variable σ_1 are shown in Figure 3. Plotting the phase spaces of nodes allows us to analyze how asymmetry in coupling strength affects neurons' dynamics. As can be seen in both figures, the trajectories are the same under equal coupling strengths. As the couplings become more asymmetric, the trajectories of each layer become different. Increasing the asymmetries between coupling can change the dynamics of the layers and lead to periodic oscillations or even quiescent.

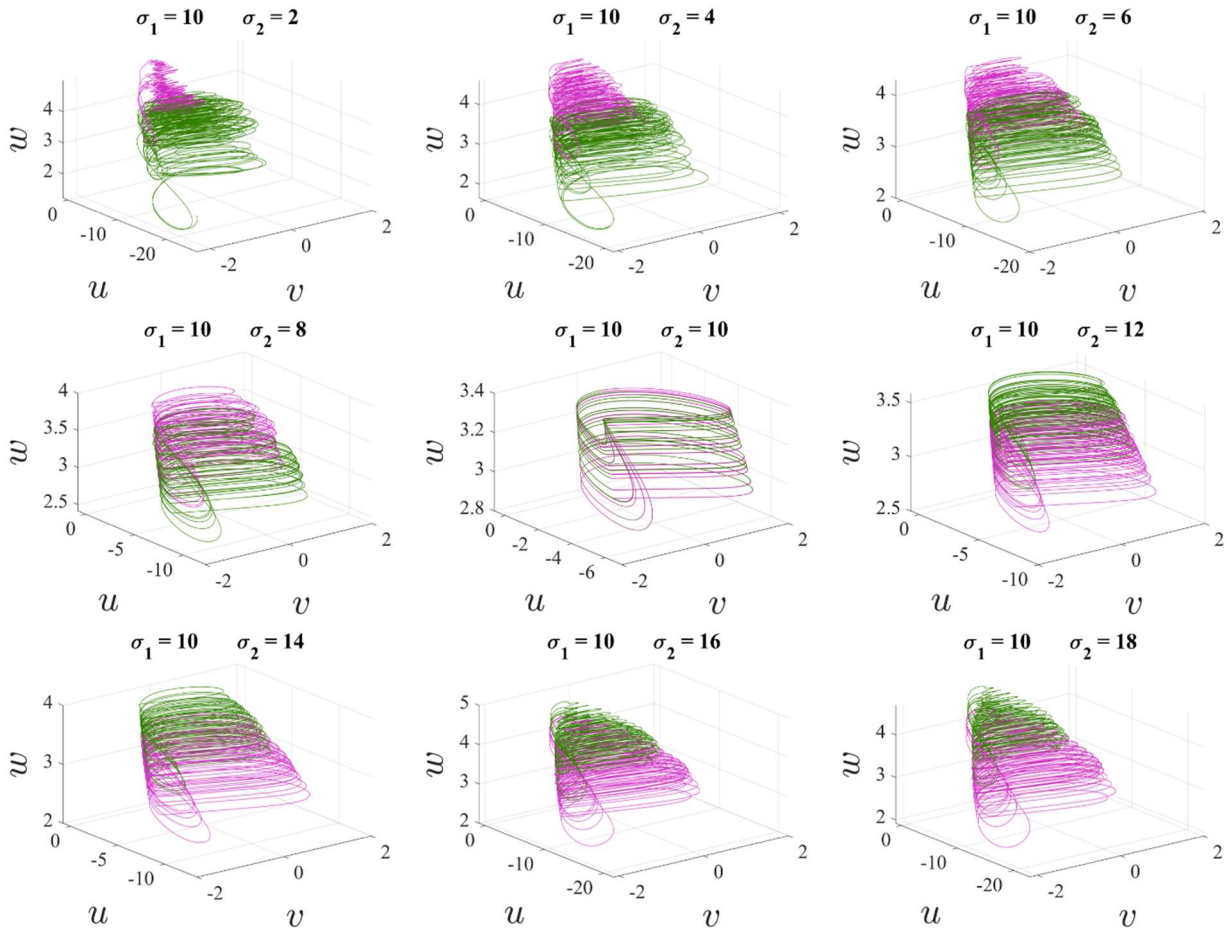

Figure 2. 3-D phase spaces of the network layers projection with fixed σ_1 and different σ_2. The pink trajectories represent neural behaviors in the left layer of the model ($L = 1$), and the green ones indicate neurons in the right layer ($L = 2$). In the equal coupling strengths for both layers, no asymmetry in trajectories is seen; however, as asymmetry arises in the coupling, the asymmetry between layers' trajectories can be seen. Hence, asymmetry coupling induces coexisting.

As variations in coupling strength result in different attractors in the layers, the bifurcation diagrams of nodes are plotted as a function of σ_1 for both layers. Figure 4 illustrates the maximum potential of the first node of each layer by varying σ_1 for some fixed σ_2. The pink diagrams illustrate the maximum voltage of the first node of layer $L = 1$, and the green diagrams illustrate the voltage of the first node of layer $L = 2$. It can be seen that changing the coupling strength alters the network dynamics. As shown in Figure 4(a) (for fixed $\sigma_2 = 0.1$), when σ_1 increases and more asymmetry occurs in the coupling, the dynamics of the layer $L = 1$ changes and finally become periodic. The periodic region emerges for $\sigma_1 > 1.79$. Moreover, the maximum amplitude of the neurons of layer $L = 1$ decreases. In this case, the dynamics of the second layer are not changed significantly. Figure 4(b),(c) depict results for larger σ_2, $\sigma_2 = 1$, and $\sigma_2 = 5$, respectively. As it can be seen, for larger σ_2, the variation in the dynamics of the second layer is more remarkable. Similar to Figure 4(a), for $\sigma_2 = 1$, the maximum amplitude of the neurons of layer $L = 1$ is decreased by increasing σ_1. Although in most couplings, the behavior is chaotic, in Figure 4(c), a periodic window can be seen for $7.58 < \sigma_1 <$

8.18 for the first neuron of both layers. Figure 4(d) shows the bifurcations for $\sigma_2 = 10$. Here, more periodic windows can be seen for both layers. The biggest ones in $L = 1$ and $L = 2$ are $6.56 < \sigma_1 < 8.02$ and $6.67 < \sigma_1 < 8.02$, respectively. Maximum amplitude values of the first node in layer $L = 1$ do not seem to change drastically; however, the one in layer $L = 2$ increases at first and then remains constant.

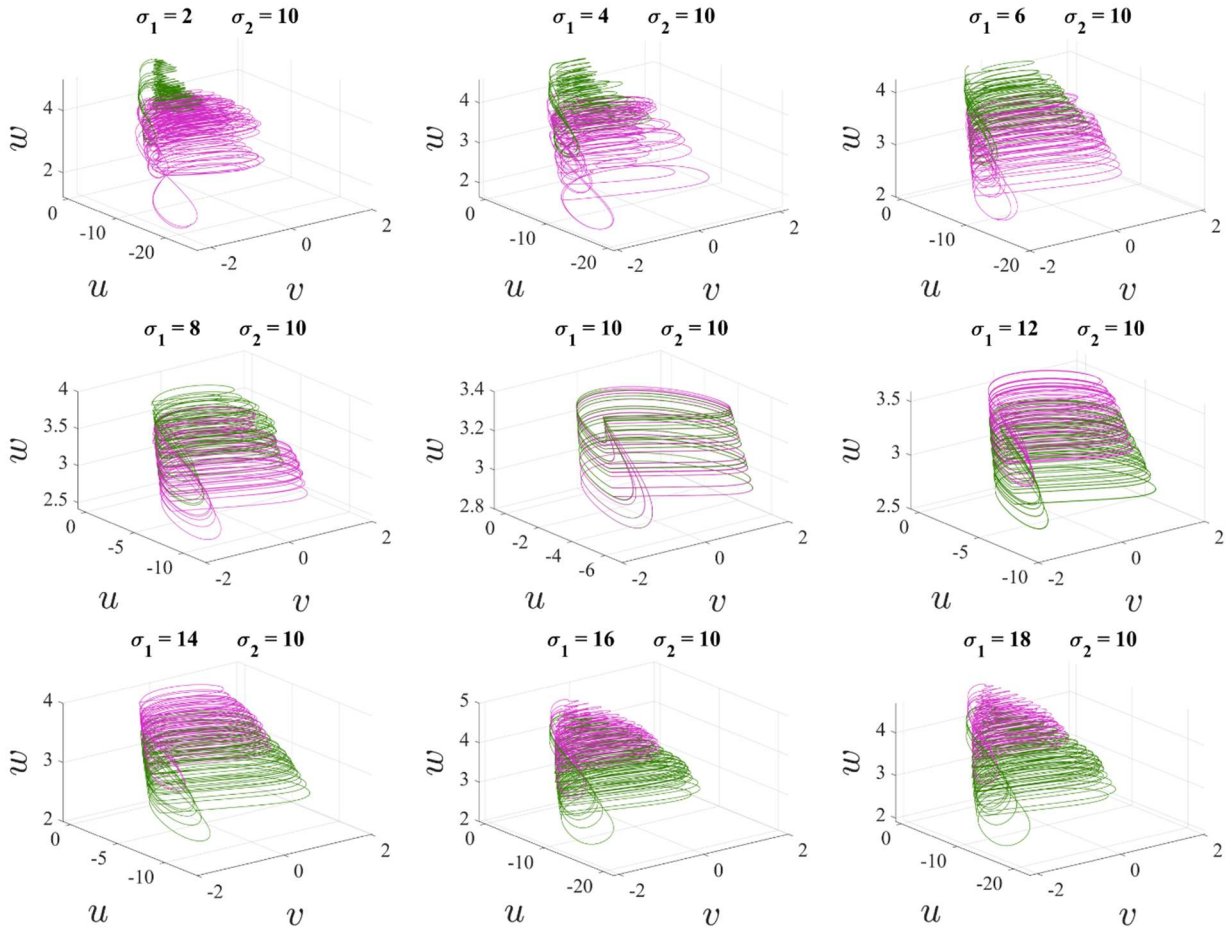

Figure 3. 3-D phase spaces of the network layers projection with fixed σ_2 and different σ_1. The pink trajectories represent neural behaviors in the left layer of the model, and the green ones indicate neurons in the right layer. No asymmetry in trajectories is seen in the equal coupling strengths for both layers. However, as asymmetry arises in the coupling, the asymmetry between layers' trajectories can be seen. Hence, asymmetry coupling induces coexisting.

Network behaviors can also be better understood by evaluating synchronization, which is obtained by computing intra-layer (Err_1 and Err_2) and inter-layer (Err) errors through Eq (3).

$$Err_1 = \langle \frac{1}{N-1} \sum_{i=2}^{N} \sqrt{\left(X_{1,1} - X_{1,i}\right)^2} \rangle_t , \forall\, X \in \{v, u, w\} \tag{3-a}$$

$$Err_2 = \langle \frac{1}{N-1} \sum_{i=2}^{N} \sqrt{\left(X_{2,1} - X_{2,i}\right)^2} \rangle_t , \forall\, X \in \{v, u, w\} \tag{3-b}$$

$$Err = \langle \frac{1}{N} \sum_{i=2}^{N} \quad \sqrt{\left(X_{2,i} - X_{1,i}\right)^2} \rangle_t \, , \forall \, X \in \{v, u, w\} \tag{3-c}$$

As shown in Figure 5, each error is calculated in the $\sigma_1 - \sigma_2$ plane and color bars indicate the error values. As a result of choosing large σ_2 and small σ_1 (e.g., $\sigma_1 = 1.1$ and $\sigma_2 = 12$), the intra-layer error of layer $L = 1$ is significantly larger compared to the opposite choices. In the case of Err_2, the result is completely opposite. Both intra-layer errors tend to be zero as asymmetry fades. The minimum error can be obtained when $\sigma_1 = \sigma_2$. The result is the same for interlayer error, although in this case, any asymmetry in coupling enlarges the error.

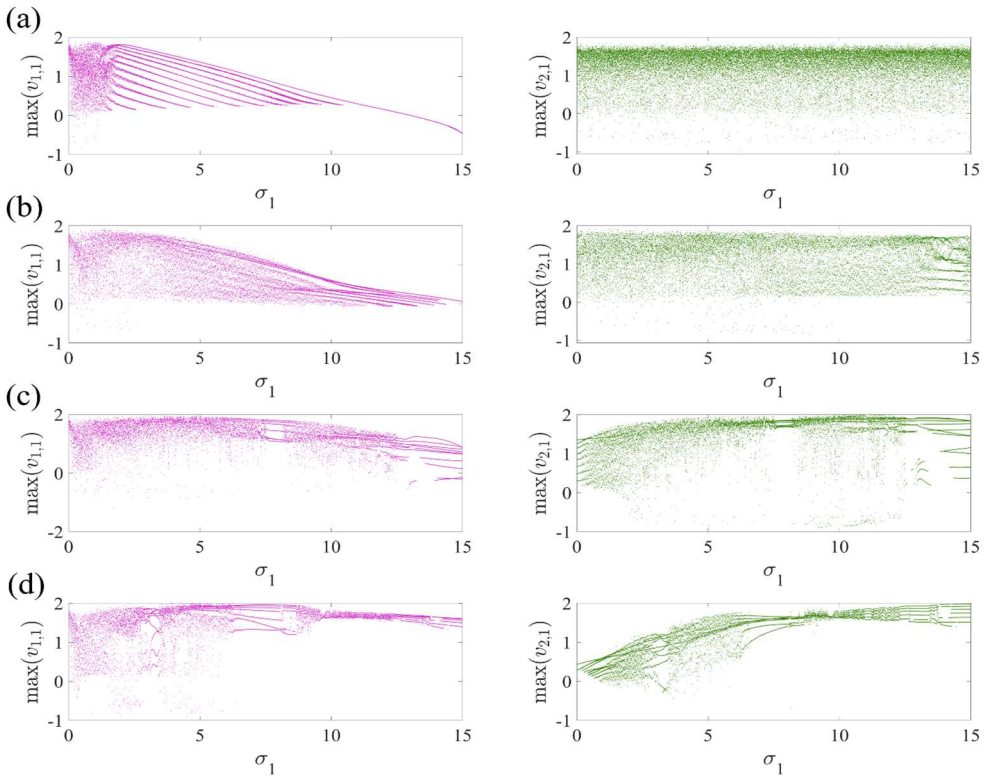

Figure 4. The bifurcation diagram of $v_{1,1}$ (left panel) and $v_{2,1}$ (right panel) vs σ_1 for $\sigma_2 = 0.1$ (a), $\sigma_2 = 1$ (b), $\sigma_2 = 5$ (c), and $\sigma_2 = 10$ (d). Dynamics vary as a result of variations in coupling. Chaotic and periodic oscillation in all diagrams can be seen.

Also, Figure 6 shows errors as a function of σ_1 for some fixed σ_2. When σ_2 is chosen as $\sigma_1 \leq 1$, errors cannot be precisely equal to zero in the symmetry case ($\sigma_1 = \sigma_2$). However, the minimum Err occurs at those points. In Figure 6(a), more asymmetry reduces Err_1 while a similar pattern could not be observed in Err_2. Based on its bifurcation diagram in Figure 4(a), it appears that in $\sigma_1 = 0.1$ and $\sigma_2 > 1.79$, neurons oscillate periodically in $L = 1$ and chaotically in $L = 2$. Hence, there is a reduction in Err_1 that reflects the ordered dynamics in the layer. Figure 6-b shows that the error trend tends to be the same, whereas in this case, when Err_1 reduces, Err_2 increases, and as a result, Err increases. When σ_2 is set to larger values as in Figure 6(c),(d), the minimum errors are found for the symmetric coupling. Furthermore, compared to the corresponding bifurcations (Figure 4(c),(d)), for those couplings that place the neuron within the periodic window, the errors are somewhat reduced (which can be seen for $\sigma_2 = 5$).

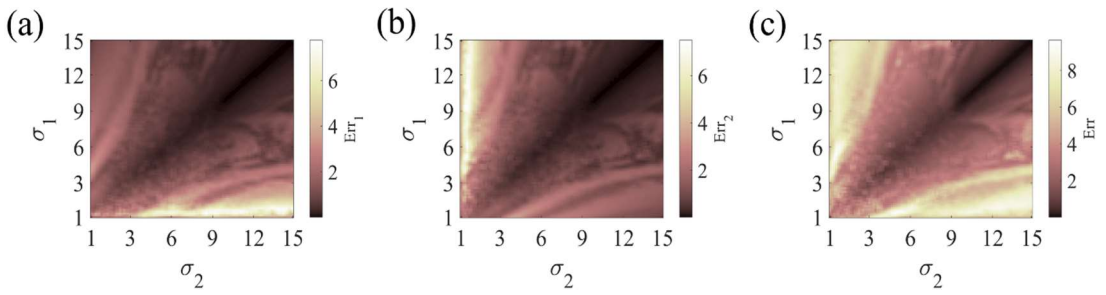

Figure 5. Intra-layer (a-b) and inter-layer (c) errors in the $\sigma_1 - \sigma_2$ planes. Color bars indicate the error value of the panel. In each plane, darker colors represent lower errors, and black illustrates the near-zero error. When the coupling asymmetry decreases, the errors decrease as well. As compared to choosing the opposite value, (a) leads to the largest error when σ_2 is large and σ_1 is small, and (b) has the opposite result; however, any asymmetry in (c) enlarges the total error.

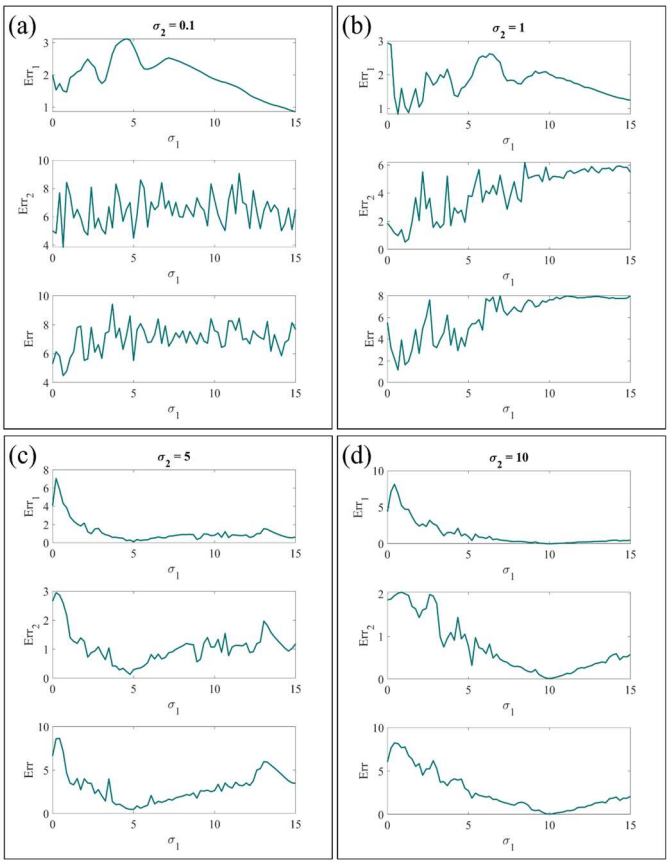

Figure 6. Intra-layer (Err_1 and Err_2) and inter-layer (Err) errors versus σ_1 for $\sigma_2 = 0.1$ (a), $\sigma_2 = 1$ (b), $\sigma_2 = 5$ (c) and $\sigma_2 = 10$ (d). Generally, the tendency for errors to decrease to zero is stronger in more symmetric couplings. Errors declination can also be caused by neuron placement in periodic dynamics regions due to changes in coupling strength. Comparing errors for different coupling strengths shows that symmetry can lead to lower errors between layers of the multi-layer network when the coupling strength is large enough.

4. Conclusions

Asymmetry is an essential phenomenon that participates in different brain performances. In this study, we considered a multi-layer network with two layers, each one as a mini model of one brain hemisphere. This viewpoint examined the effect of asymmetry in coupling strength, which led to asymmetry in the trajectories. The HR model was used as the dynamics of each node. For each layer, a different coupling was used for connecting its nodes. Then, the dynamics of the multi-layer network were examined in the phase space. Despite the absence of coexisting attractors in the HR model, asymmetry in couplings led to various attractors in the network. For better analyses, the bifurcation diagrams of the first node of each layer were plotted as a function of one coupling strength while the other one was chosen fixed. Moreover, intra-layer and inter-layer errors of neurons were calculated to investigate the synchronization of the network. Errors were almost equal to zero for symmetric couplings that were large enough.

Acknowledgments

This work is partially funded by Centre for Nonlinear Systems, Chennai Institute of Technology, India vide funding number CIT/CNS/2022/RD/006. The work and the contribution were also supported by the SPEV project, University of Hradec Kralove, Faculty of Informatics and Management, Czech Republic (ID: 2102–2022), "Smart Solutions in Ubiquitous Computing Environments". We are also grateful for the support of student Michal Dobrovolny in consultations regarding application aspects.

Conflict of interest

The authors declare that there is no conflict of interest.

References

1. F. Parastesh, S. Jafari, H. Azarnoush, Z. Shahriari, Z. Wang, S. Boccaletti, et al., Chimeras, *Phys. Rep.*, **898** (2021), 1–114. https://doi.org/10.1016/j.physrep.2020.10.003
2. S. Majhi, B. K. Bera, D. Ghosh, M. Perc, Chimera states in neuronal networks: A review, *Phys. Life Rev.*, **28** (2019), 100–121. https://doi.org/10.1016/j.plrev.2018.09.003
3. F. Parastesh, M. Mehrabbeik, K. Rajagopal, S. Jafari, M. Perc, Synchronization in Hindmarsh-Rose neurons subject to higher-order interactions, *Chaos*, **32** (2022), 013125. https://doi.org/10.1063/5.0079834
4. K. Rajagopal, S. He, A. Karthikeyan, P. Duraisamy, Size matters: Effects of the size of heterogeneity on the wave re-entry and spiral wave formation in an excitable media, *Chaos*, **31** (2021), 053131. https://doi.org/10.1063/5.0051010
5. Z. Wang, Z. Rostami, S. Jafari, F. E. Alsaadi, M. Slavinec, M. Perc, Suppression of spiral wave turbulence by means of periodic plane waves in two-layer excitable media, *Chaos Solitons Fractals*, **128** (2019), 229–233. https://doi.org/10.1016/j.chaos.2019.07.045
6. Z. Yao, C. Wang, P. Zhou, J. Ma, Regulating synchronous patterns in neurons and networks via field coupling, *Commun. Nonlinear Sci. Numer. Simul.*, **95** (2021), 105583. https://doi.org/10.1016/j.cnsns.2020.105583

7. Z. Yao, C. Wang, Control the collective behaviors in a functional neural network, *Chaos Solitons Fractals*, **152** (2021),111361. https://doi.org/10.1016/j.chaos.2021.111361
8. P. Zhou, X. Zhang, X. Hu, G. Ren, Energy balance between two thermosensitive circuits under field coupling, *Nonlinear Dyn.*, **110** (2022), 1879–1895. https://doi.org/10.1007/s11071-022-07669-z
9. N. Naseri, F. Parastesh, F. Ghassemi, S. Jafari, E. Schöll, J. Kurths, Converting high dimensional complex networks to lower dimensional ones preserving synchronization features, *Eur. Lett.*, **140** (2022), 21001. https://doi.org/10.1209/0295-5075/ac98de
10. V. Thibeault, G. St-Onge, L. J. Dubé, P. Desrosiers, Threefold way to the dimension reduction of dynamics on networks: An application to synchronization, *Phys. Rev. Res.*, **2** (2020), 043215. https://doi.org/10.1103/PhysRevResearch.2.043215
11. Q. Xu, T. Liu, S. Ding, H. Bao, Z. Li, B. Chen, Extreme multistability and phase synchronization in a heterogeneous bi-neuron Rulkov network with memristive electromagnetic induction, *Cogn. Neurodyn.*, **2022** (2022), 1–12. https://doi.org/10.1007/s11571-022-09866-3
12. Q. Xu, X. Tan, D. Zhu, M. Chen, J. Zhou, H. Wu, Synchronous behavior for memristive synapse-connected Chay twin-neuron network and hardware implementation, *Math. Probl. Eng.*, **2020** (2022), 8218740. https://doi.org/10.1155/2020/8218740
13. S. Rakshit, S. Majhi, J. Kurths, D. Ghosh, Neuronal synchronization in long-range time-varying networks, *Chaos*, **31** (2021), 073129. https://doi.org/10.1063/5.0057276
14. K. Clark, R. F. Squire, Y. Merrikhi, B. Noudoost, Visual attention: Linking prefrontal sources to neuronal and behavioral correlates, *Prog. Neurobiol.*, **132** (2015), 59–80. https://doi.org/10.1016/j.pneurobio.2015.06.006
15. Z. Bahmani, K. Clark, Y. Merrikhi, A. Mueller, W. Pettine, M. I. Vanegas, et al., Prefrontal contributions to attention and working memory, *Curr. Top Behav. Neurosci*., **41** (2019), 129–153. https://doi.org/10.1007/7854_2018_74
16. J. S. Kwon, B. F. O'Donnell, G. V. Wallenstein, R. W. Greene, Y. Hirayasu, P. G. Nestor, et al., Gamma frequency-range abnormalities to auditory stimulation in schizophrenia, *Arch. Gen. Psychiatry*, **56** (1999), 1001–1005. https://doi.org/10.1001/archpsyc.56.11.1001
17. G. G. Knyazev, J. Y. Slobodskoj-Plusnin, A. V. Bocharov, L. V. Pylkova, The default mode network and EEG alpha oscillations: An independent component analysis, *Brain Res.*, **1402** (2011), 67–79. https://doi.org/10.1016/j.brainres.2011.05.052
18. F. A. Fishburn, V. P. Murty, C. O. Hlutkowsky, C. E. MacGillivray, L. M. Bemis, M. E. Murphy, et al., Putting our heads together: interpersonal neural synchronization as a biological mechanism for shared intentionality, *Soc. Cogn. Affect. Neurosci.*, **13** (2018), 841–849. https://doi.org/10.1093/scan/nsy060
19. E. Bullmore, O. Sporns, Complex brain networks: Graph theoretical analysis of structural and functional systems, *Nat. Rev. Neurosci.*, **10** (2009), 186–198. https://doi.org/10.1038/nrn2575
20. P. Hagmann, L. Cammoun, X. Gigandet, R. Meuli, C. J. Honey, V. J. Wedeen, et al., Mapping the structural core of human cerebral cortex, *PLoS Biol.*, **6** (2008), e159. https://doi.org/10.1371/journal.pbio.0060159
21. B. P. Rogers, V. L. Morgan, A. T. Newton, J. C. Gore, Assessing functional connectivity in the human brain by fMRI, *Magn. Reson. Imaging*, **25** (2007), 1347–1357. https://doi.org/10.1016/j.mri.2007.03.007

22. M. Gosak, M. Milojević, M. Duh, K. Skok, M. Perc, Networks behind the morphology and structural design of living systems, *Phys. Life Rev.*, **41** (2022), 1–21. https://doi.org/10.1016/j.plrev.2022.03.001
23. S. D. Glick, D. A. Ross, L. B. Hough, Lateral asymmetry of neurotransmitters in human brain, *Brain Res.*, **234** (1982), 53–63. https://doi.org/10.1016/0006-8993(82)90472-3
24. L. Tian, J. Wang, C. Yan, Y. He, Hemisphere-and gender-related differences in small-world brain networks: a resting-state functional MRI study, *Neuroimage*, **54** (2011), 191–202. https://doi.org/10.1016/j.neuroimage.2010.07.066
25. S. F. Witelson, D. L. Kigar, Sylvian fissure morphology and asymmetry in men and women: bilateral differences in relation to handedness in men, *J. Comp. Neurol.*, **323** (1992), 326–340. https://doi.org/10.1002/cne.903230303
26. L. Jäncke, G. Schlaug, Y. Huang, H. Steinmetz, Asymmetry of the planum parietale, *Neuroreport*, **5** (1994), 1161–1163. https://psycnet.apa.org/doi/10.1097/00001756-199405000-00035
27. G. W. Hynd, M. Semrud-Clikeman, A. R. Lorys, E. S. Novey, D. Eliopulos, Brain morphology in developmental dyslexia and attention deficit disorder/hyperactivity, *Arch. Neurol.*, **47** (1990), 919–926. https://doi.org/10.1001/archneur.1990.00530080107018
28. R. M. Bilder, H. Wu, B. Bogerts, M. Ashtari, D. Robinson, M. Woerner, et al., Cerebral volume asymmetries in schizophrenia and mood disorders: A quantitative magnetic resonance imaging study, *Int. J. Psychophysiol.*, **34** (1999), 197–205. https://doi.org/10.1016/S0167-8760(99)00077-X
29. P. M. Thompson, J. Moussai, S. Zohoori, A. Goldkorn, A. A. Khan, M. S. Mega, et al., Cortical variability and asymmetry in normal aging and Alzheimer's disease, *Cereb. Cortex*, **8** (1998), 492–509. https://doi.org/10.1093/cercor/8.6.492
30. S. Rakshit, F. Parastesh, S. N. Chowdhury, S. Jafari, J. Kurths, D. Ghosh, Relay interlayer synchronisation: invariance and stability conditions, *Nonlinearity*, **35** (2021), 681. https://doi.org/10.1088/1361-6544/ac3c2f
31. E. S. Medeiros, U. Feudel, A. Zakharova, Asymmetry-induced order in multilayer networks, *Phys. Rev. E*, **104** (2021), 024302. https://doi.org/10.1103/PhysRevE.104.024302
32. B. M. Tijms, A. M. Wink, W. de Haan, W. M. van der Flier, C. J. Stam, P. Scheltens, et al., Alzheimer's disease: Connecting findings from graph theoretical studies of brain networks, *Neurobiol. Aging*, **34** (2013), 2023–2036. https://doi.org/10.1016/j.neurobiolaging.2013.02.020
33. S. Majhi, M. Perc, D. Ghosh, Dynamics on higher-order networks: A review, *J. R. Soc. Interface*, **19** (2022), 20220043. https://doi.org/10.1098/rsif.2022.0043
34. M. De Domenico, A. Solé-Ribalta, E. Cozzo, M. Kivelä, Y. Moreno, M. A. Porter, et al., Mathematical formulation of multilayer networks, *Phys. Rev. X*, **3** (2013), 041022. https://doi.org/10.1103/PhysRevX.3.041022
35. F. Battiston, V. Nicosia, M. Chavez, V. Latora, Multilayer motif analysis of brain networks, *Chaos*, **27** (2017), 047404. https://doi.org/10.1063/1.4979282
36. A. Karthikeyan, I. Moroz, K. Rajagopal, P. Duraisamy, Effect of temperature sensitive ion channels on the single and multilayer network behavior of an excitable media with electromagnetic induction, *Chaos Solitons Fractals*, **150** (2021), 111144. https://doi.org/10.1016/j.chaos.2021.111144

37. M. Yu, M. M. A. Engels, A. Hillebrand, E. C. W. Van Straaten, A. A. Gouw, C. Teunissen, et al., Selective impairment of hippocampus and posterior hub areas in Alzheimer's disease: An MEG-based multiplex network study, *Brain*, **140** (2017), 1466–1485. https://doi.org/10.1093/brain/awx050
38. L. Kang, C. Tian, S. Huo, Z. Liu, A two-layered brain network model and its chimera state, *Sci. Rep.*, **9** (2019), 14389. https://doi.org/10.1038/s41598-019-50969-5

Appendix

The MATLAB codes used for simulations can be found from: https://drive.google.com/file/d/1AtbEvrTsJm2CTWSNp272WnasIe85ipk5/view?usp=share_link.

AIMS Press